

## Cu:Si(111) incommensurate ( $5.55 \times 5.55$ ) surface reconstruction: Helium-beam measurements of diffraction and surface phonons

R. B. Doak and D. B. Nguyen

*AT&T Bell Laboratories, Murray Hill, New Jersey 07974-2070*

(Received 27 December 1988)

Elastic and inelastic atomic-helium scattering has been used to characterize the Cu:Si(111) “quasi- $(5 \times 5)$ ” surface. The surface superlattice is incommensurate with the underlying Si(111) structure, 5.55 times larger, appears to be limited to the outermost layers, yet is not a simple incommensurate overlayer. The helium diffraction indicates a long-range coherence of the reconstruction which, while not incompatible with a two-dimensional quasicrystal, would severely restrict any quasicrystal correlation or tiling rules. The surface phonons have intriguing characteristics including a lack of band gaps at fractional-order “zone boundaries” and what seems to be a continuous transition from extended mode to local oscillator mode with increasing wave vector.

### INTRODUCTION

The Cu:Si(111) “quasi- $(5 \times 5)$ ” seems to defy facile insertion into any of the standard categories of surface overlayer structures. Formed by deposition of up to roughly 1 ML of copper onto Si(111) at elevated temperatures (typically 600–800 °C), the structure originally was thought to be a simple impurity-induced  $5 \times 5$  reconstruction.<sup>1</sup> Detailed low-energy electron diffraction (LEED) measurements later showed the “ $5 \times 5$ ” satellite peaks to in fact *not* lie at  $5 \times 5$  positions but rather at positions intermediate to a  $5 \times 5$  and a  $6 \times 6$  reconstruction,<sup>2,3</sup> indicating an *incommensurate* superstructure  $5\frac{1}{2}$  times larger than a Si(111)- $(1 \times 1)$  unit cell. Examination of LEED intensities<sup>2</sup> as a function of electron energy further suggested that the surface was *not* a simple incommensurate overlayer such as formed, for example, by rare gases on graphite. Scanning tunneling microscopy (STM) measurements tell a similar tale.<sup>4,5</sup> STM topographic and current tunneling images reveal a complicated conglomeration of at least three different local (atomic scale) features. Although the structure appears quite chaotic at first glance, Demuth *et al.*<sup>4</sup> have Fourier analyzed their real-space STM images and shown them to contain the same symmetries exhibited in LEED patterns. Moreover by suitably filtering their STM images prior to Fourier transforming, they have been able to associate specific real-space features with the incommensurate “quasi- $(5 \times 5)$ ” periodicity. Both STM groups suggest that a tiling of the surfaces may be involved, with one or more subunits whose edge dimensions appear to be an integral number of Si(111)- $(1 \times 1)$  spacings, varying between roughly 4 and 7. The average boundary length and/or “tile” form generated by this discrete distribution is thought to introduce the incommensurate  $5\frac{1}{2}$ -fold periodicity producing the satellite diffraction peaks. While much of this remains conjecture at present, it appears that there may be connections to two-dimensional (2D) quasicrystal structures and Penrose tilings. Certainly it is obvious that the CuSi(111) “quasi- $(5 \times 5)$ ” is an fascinating system with some rather unique attributes.

We independently ran afoul of this system through chance contamination of our sample while engaged in helium-atom scattering measurements of strong chemisorption on Si(111). That intriguing glimpse induced us to construct a Cu evaporator and undertake some properly characterized measurements of both the helium diffraction and the surface phonons of Cu:Si(111) “quasi- $(5 \times 5)$ .” We report those measurements here in abbreviated form and elsewhere in detail.<sup>6</sup> Helium diffraction provides a high resolution, strictly surface-sensitive reciprocal-space measurement (with *no* multiple scattering) for comparison with the STM Fourier power spectra.<sup>4</sup> The phonon measurements are intriguing in their own right: At long wavelengths a surface vibration is, *comparatively* speaking, less sensitive to atomic scale surface disorder than at very short (Brillouin zone boundary) wavelengths. Since Cu:Si(111) “quasi- $(5 \times 5)$ ” apparently combines a well-defined long-range *order* with a well-defined short-range *disorder*, an acoustic phonon, when measured from zone center to zone boundary, may metamorphose from an extended lattice mode to a local oscillator mode. The measured inelastic time-of-flight (TOF) peaks show characteristics consistent with this conjecture.

### EXPERIMENTAL MEASUREMENTS

Elastic and inelastic helium-atom scattering was carried out with an apparatus which has been described in detail elsewhere.<sup>7</sup> Most of these measurements were made with an incident beam energy of about  $6 \text{ \AA}^{-1}$ , rotating the target to vary the angles of incidence and emergence ( $\theta_i$  and  $\theta_f$ , respectively, measured with respect to the surface normal) under a fixed total-scattering angle of  $76.14^\circ$  (i.e.,  $\theta_i + \theta_f = 76.14$ ). The scattered beam was energy-analyzed using time-of-flight (TOF) analysis.<sup>8</sup> The beam chopper was situated upstream of the target with chopper-target and target-detector flight paths 0.479 and 1.213 m, respectively. Syton-polished Si(111) substrates were prepared by either *ex situ* Shiraki etching or *in situ* UHV sputter etching ( $\text{Ar}^+$  at 1 kV) followed by

annealing at about 920°C. Copper was deposited from a simple doubly differentially pumped effusion source located about 37 cm from the target. The cleanliness and order of the surface was carefully checked before and after deposition using LEED and Auger spectroscopy for rough qualification and helium diffraction and inelastic scattering for more sensitive characterization. The deposition process was monitored using specular helium scattering or diffraction. Except as otherwise noted, copper was deposited onto a target (at typically 650°C) just until the Si(111)-(7×7) spots had disappeared and the specular had risen and plateaued. This probably corresponds to very nearly 1 ML at saturation coverage. The total scattering angle of 76.14° was chosen to facilitate specular monitoring: At this angle destructive interference from the Si(111)-(7×7) corrugation effectively removes the specular peak, providing extraordinary sensitivity to the copper-induced changes in corrugation [the specular rises from a few kilohertz to a few megahertz as the Cu:Si(111) "quasi-(5×5)" forms].

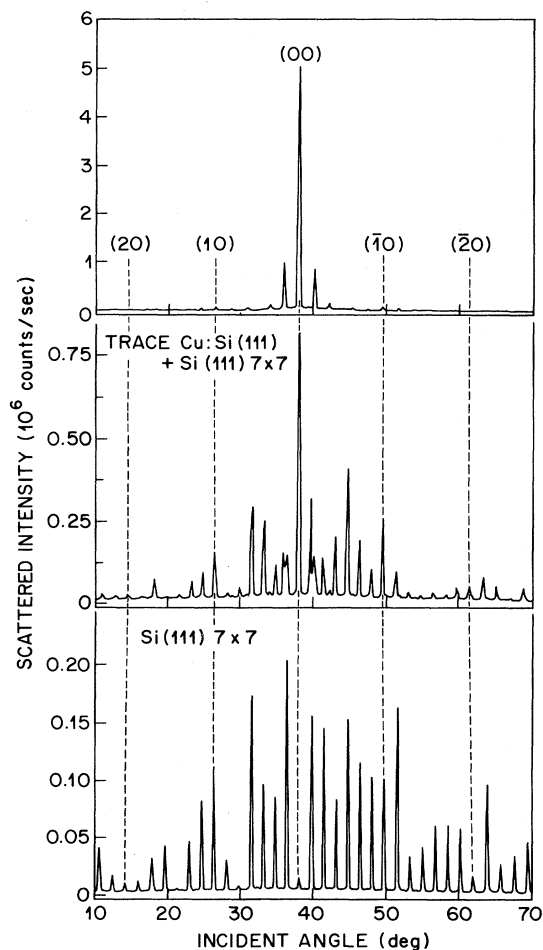


FIG. 1. Angular distributions of elastic helium scattering in the  $\langle 112 \rangle$  azimuth, total-scattering angle of 76.14°. Bottom: clean Si(111)-(7×7), incident beam wave vector  $k = 5.906 \text{ \AA}^{-1}$ . Middle: with 0.1–0.2 monolayer (ML) copper,  $k_i = 5.989 \text{ \AA}^{-1}$ . Top: saturated Cu:Si(111)-(5.55×5.55) with approximately 1 ML of copper,  $k_i = 6.012 \text{ \AA}^{-1}$ .

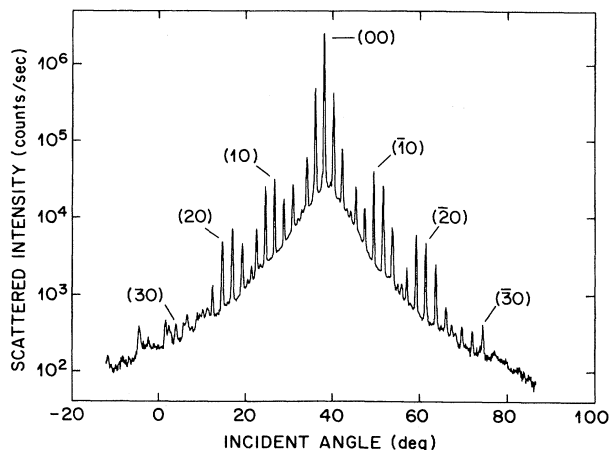


FIG. 2. Cu:Si(111)-(5.55×5.55) diffraction scan. Same as Fig. 1 (top) but plotted on a semilog scale.

## RESULTS

Virtually any amount of copper on the Si(111) surface produced a readily identifiable diffraction signature (Fig. 1). At low coverages this was mixed with diffraction from the Si(111)-(7×7) structure. With increasing copper exposure the seventh-order spots diminished and were eventually fully extinguished. Copper thus appears to be highly mobile at the deposition temperature ( $\sim 650^\circ\text{C}$ ) and to island at very low coverage. As shown in Fig. 1, elastic scattering from Cu:Si(111) is dominated by the specular and by the first few "fifth"-order spots. If the ordinate is expanded, however, as in the semilog plot of Fig. 2, it is clear that a well-defined hierarchy of diffraction spots exists. The *in situ* variable flight path of the present apparatus allows us to measure the incident beam wave vector extremely accurately<sup>7,8</sup> and to calculate reciprocal lattice vectors to correspondingly high absolute precision. A least-squares fit<sup>8</sup> to the six integer

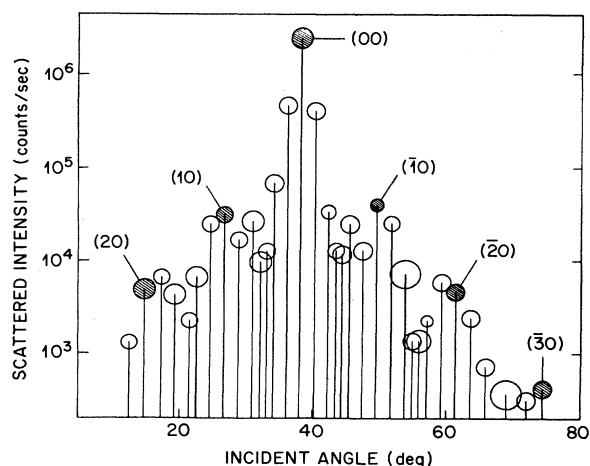


FIG. 3. Relative angular widths (FWHM) of diffraction peaks, coded as diameter of circles. Overall average width is 0.30°. Integer order circles are shaded.

peaks and specular of Fig. 2 yielded  $G(10)=1.8930 \pm 0.0078 \text{ \AA}^{-1}$ . About half of the error bar is statistical, the remainder arises through conservative assigned systematic error bars of  $\pm 0.2^\circ$  and  $\pm 0.02 \text{ \AA}^{-1}$  for the total-scattering angle and incident beam wave vector, respectively. For comparison, the accepted Si bulk value is  $1.8893 \text{ \AA}^{-1}$ . It thus appears that the integer order periodicity is exactly that of the Si(111) substrate.

Surrounding each integer order peak is an envelope of "fifth"-order satellite peaks. Three of these are generally apparent to each side of an integer order peak, with envelopes overlapping such that the third satellite in each series interposes itself between the second and third satellites of the adjacent series, i.e., starting with (00) and moving to smaller  $\theta$ : (00), (00) + " $\frac{1}{5}$ ," (00) + " $\frac{2}{5}$ ," (10) - " $\frac{3}{5}$ ," (00) + " $\frac{3}{5}$ ," (10) - " $\frac{2}{5}$ ," etc. All diffraction intensities, integer and satellite, are fairly symmetric about the specular [note that the (7×7) diffraction, Fig. 1, is *not*]. The envelope of peak intensities about each integer spots shows roughly the same trend: The first satellite is larger than the second (note the logarithmic ordinate in Fig. 2) which in turn is much larger than the third. Of interest also is the width of each of these diffraction peaks. This is depicted in Fig. 3, with the width (FWHM) coded as the diameter of each circle. The satellites may be slightly broader than the integer peaks but the difference does not appear to be statistically significant. Overall the average peak width is about  $0.30^\circ$ , comparable to (perhaps slightly larger) than that obtained with cleaved surfaces (e.g., LiF) known to give large perfect domains. TOF spectra at the satellite angles shows that they are without doubt, due to elastic scattering.

Defining the "proper" fractional reciprocal lattice vector (see below) to be that connecting the integer peak and adjacent satellite peak, we then put a least-squares fit

through the satellite angles comprising the envelopes surrounding the (00), ( $\pm 10$ ), and ( $\pm 20$ ) peaks<sup>6</sup> and extracted the fractional vector for each set. Averaging these values yielded  $G(\frac{1}{5}, 0) = 0.3407 \pm 0.0023 \text{ \AA}^{-1}$ . Incorporating the same systematic error bars as above raises this uncertainty to  $\pm 0.0026 \text{ \AA}^{-1}$ . To this degree of accuracy there were no discernible systematic trends among the residuals of the least-squares fits. Diffraction in the  $\langle 110 \rangle$  azimuth yielded compatible values. Based on the measured integer order reciprocal vector quoted above, the supercell is thus  $5.55 \pm 0.05$  larger than a (1×1) unit cell.

In addition to this elastic scattering, we carried out extensive *inelastic* helium scattering measurements. Details of the TOF spectra are presented elsewhere,<sup>6</sup> and we summarize the measured surface phonon dispersion curves in the extended zone plot of Fig. 4. Of particular interest is the existence of Rayleigh-like acoustic branches associated with the fractional order diffraction channels as well as the integer channels. The inelastic TOF peaks corresponding to all of the Rayleigh modes are sharp and intense near zero energy (i.e., at long wavelength) and broaden from sub-meV to multiple-meV widths as they are tracked to higher energies (shorter wavelengths). Eventually these signatures merge into the broad "Einstein-like" mode near 8 meV indicated by the dotted line. Higher harmonics, or overtones, of this broad flat mode are also seen.

## DISCUSSION

Since helium atoms do not penetrate into the surface, it is impossible to "mix" diffraction peaks from the outermost layer with those from deeper layers as often produces satellite peaks with LEED. The helium diffraction pattern of Fig. 2 is therefore truly representative of the surface corrugation, and we eliminate as a possibility, on that basis, a simple incommensurate overlayer structure (such as found with rare gases on graphite) as the source of the satellites. A related question concerns the correct periodicity of the surface structure: Clearly this set of diffraction peaks could be generated by a reciprocal lattice vector of either  $0.341 \text{ \AA}^{-1}$ , as discussed above, or  $1.889 \pm 0.341 = 1.548$  or  $2.230 \text{ \AA}^{-1}$ , the difference being that of a supercell 5.55, as opposed to 1.22 or 0.85 times larger than the Si(111)-(1×1), respectively. The issue is not clear cut here. We are inclined to argue, however, that the rapid decrease in diffraction intensity with momentum transfer allows us to eliminate the latter possibilities. Namely the larger fractional reciprocal vectors would require, for each satellite, an admixture with the next integer channel for which, as seen in Fig. 2, the intensity is typically an order of magnitude *less* than the *satellite itself*. We thus believe the 5.55 supercell is the correct assignment. In all events we find only a *single* periodicity of reconstruction to within stringent error bars.

With this assignment, a coherent picture emerges upon considering the intensity and width of the diffraction features. There is an overall exponential decay in diffraction intensities upon moving out from the specular, reminiscent of the situation invariably encountered with

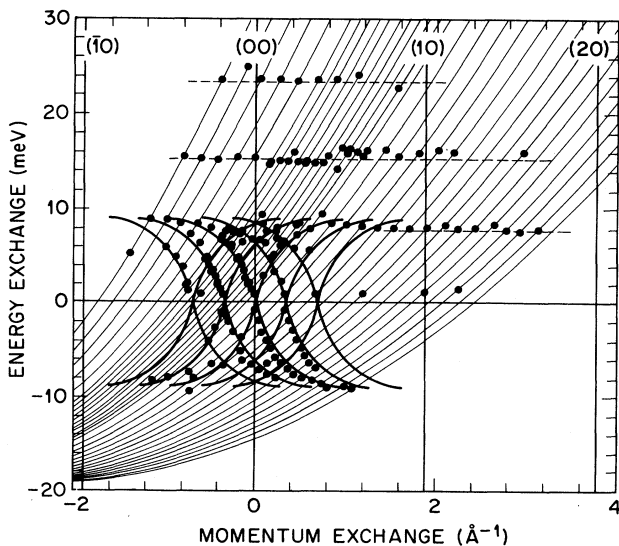


FIG. 4. Measured surface phonon dispersion curves for Cu:Si(111)-(5.55×5.55),  $\langle 112 \rangle$  azimuth. Solid lines are rough fits to the Rayleigh dispersion curves, dashed lines are broad flat modes. Parabolic lines are scan curves.

smooth metal surfaces. We believe the underlying cause is the same, a very shallow corrugation due to the smoothing presence of free electrons. STM measurements agree,<sup>5</sup> showing a surface corrugation of only about 0.2 Å with that technique.

Superimposed upon this overall decline is an envelope of satellite intensities centered at each integer-order position, as discussed above. This envelope is of particular interest as it represents, in essence, the Fourier transform of the real-space disturbance producing the  $5.55 \times 5.55$  pattern. In a two-component system substitutional disorder is a very real possibility, and one might assign the 5.55 periodicity to an incommensurate substitutional disorder<sup>9</sup> or combination of substitutional and displacement disorder.<sup>9</sup> The STM measurements rule out a simple, smoothly varying incommensuration. However, as Guinier shows,<sup>9</sup> two successive sequences of differently spaced lattice rows within the supercell will yield a similar satellite structure (in effect the Fourier transform of a square-wave disturbance and, as seen in Fig. 2, the necessary higher-order satellite reciprocal wave vectors are indeed present). In this sense the diffraction features are completely consistent with a Frenkel-Kontorova—Frank—Van der Merwe<sup>10</sup> “tiling” of subunits based upon relaxation of adsorbate-induced surface stress as discussed by Wilson and Chiang.<sup>5</sup> The immediate question is then whether the disorder apparent in a STM photo is due simply to defects in an ideal  $5.55 \times 5.55$  lattice or whether an underlying  $5.55 \times 5.55$  quasicrystal structure is present. More recent STM current image work by Demuth and colleagues<sup>11</sup> would indicate the latter. In particular, patterns similar to their distribution of “deep triangular rings” can be generated by decoration of the Si(111)-(1×1) template according to a few simple correlation rules.<sup>6</sup> The sharpness of the helium-diffraction peaks severely limits the choice of these correlation rules. Our 0.3° FWHM corresponds to an instrumental transfer width of some 100 Å,<sup>12</sup> indicating that the coherence length on the surface is at least this large, or many supercells in extent. It would seem that any correlation rules must therefore be *global* rather than *local* in nature. In Guinier’s terminology<sup>9</sup> this is a crystal imperfection of the first rather than the second type. Simple Markovian processes alone are inadequate. Generating the superlattice by randomly placing each successive crater four to seven silicon lattice spacings removed from an existing neighbor is insufficiently stringent. Either higher-order correlations must be introduced (e.g., a spacing of four can be followed only by a spacing of six or seven, etc.), or the “tiling” must be of specific *shapes* rather than boundaries (Penrose-like tiling) or the correlation rules must be strictly global [generate a  $5\frac{1}{2} \times 5\frac{1}{2}$  lattice on top of the (1×1) and place craters by random choice at one of the nearest (1×1) lattice sites adjacent to each  $5\frac{1}{2}$ -fold point]. Kuo *et al.*<sup>13</sup> have discussed the hierarchy of such correlation rules in conjunction with the growth of 3D quasicrystals. We mention also that in the case of a *discrete* tiling on a Si(111)-(1×1) substrate, the width of the satellite intensity envelope should reflect the average variation of boundary length/tile dimension. The results of Fig. 2 would appear to be in close agreement with the

distribution of four to seven (1×1) spacings seen with STM.<sup>4,11</sup> In summary, we feel that it is entirely possible for the Cu:Si(111)-(5.55×5.55) to arise through a quasicrystal tiling on the Si(111)-(1×1) template but that neither the STM nor the helium diffraction rule out all other possibilities, for example a defected incommensurate lattice of domain walls.

Finally, we close with a brief mention of the surface phonons. Nearly all of the coherent scattering comes out in the specular channel (Fig. 1) with correspondingly intense specular phonon sidebands. Considerable surface disorder is indicated by the substantial incoherent elastic peak (two to ten times larger than the phonon peaks) but the integrated single phonon intensity still accounts for the majority of the scattered intensity at any nondiffraction angle.

To the best of our knowledge, these are the first phonon measurements in an incommensurate surface, in which regard the Rayleigh phonon branches associated with the fractional order rods bear particular scrutiny. These are umklapp processes via an incommensurate reciprocal-lattice vector. The inelastic TOF peaks corresponding to these fractional order branches appear in no way extraordinary. Their intensities are lower than those of the specular Rayleigh mode but by about the ratio of respective diffraction intensities, as expected. The fractional order peaks may be slightly broader in energy but only marginally so. To within the instrumental energy resolution, the fractional order Rayleigh modes drop completely to zero frequency at the fractional lattice positions. Surprisingly, though, *no* band gap exists at the intersection of fractional and specular order modes (this is not obvious from Fig. 4, but a plot of TOF intensities<sup>6</sup> makes it quite clear). We feel this quandry may be resolved if the incommensurate structure is limited to the outermost layer (or a *very* few layers) of the crystal. Since the Rayleigh mode is still deeply penetrating (about ten layers) at the intersection points, the surface structure might then perturb the phonon characteristics only slightly, even while the corrugation is sufficient to induce substantial diffraction. In effect momentum transfer due to fractional order diffraction is decoupled from that due to Rayleigh phonon excitation or deexcitation, shifting the dispersion curve by one fractional reciprocal lattice vector but not perturbing it. The surface structure is strictly 2D but the surface phonon (at this wave vector) perhaps is not. In intersections at larger wave vectors we would expect band gaps to open up. Unfortunately the rapid decline in diffraction intensity with diffraction order in the present case does not permit us to test this directly.

Finally, we remark that the broad flat band at about 8 meV is very reminiscent of a similar flat mode at 10.5 meV observed by Harten *et al.*<sup>14</sup> in clean Si(111)-(2×1) and initially characterized as an Einstein oscillator mode. Alerhand and Mele subsequently advanced an alternative theory<sup>15</sup> based upon strong electron-phonon coupling involving transitions across an indirect band gap between the zone-center back-bond orbital and an empty zone boundary surface state. This could soften the transverse acoustic mode, pulling it down into an avoided crossing

with the Rayleigh mode and yielding the measured flat mode. In the Cu:Si(111) system, with a much different surface topography and different surface electronic states, the above explanation is probably inapplicable. We thus feel that our broad 8-meV flat mode (with the two higher harmonics or overtones) is inarguably a localized Einstein oscillator mode induced by the copper and/or by the atomic-scale disorder. The flip side of this is then to ask whether controlled surface disorder might, in fact, produce a similar broad flat mode even on a clean surface such as Si(111)-(2×1).

More generally, the question is whether Cu:Si(111)-

(5.55×5.55) is unique. Our feeling is that it is not. Indeed measurements on Ga:Si(111) (Ref. 16) have already indicated that similar structures may be obtained in that system, and we expect the list to grow. In the end, an investigation of similar systems may prove the quickest method of answering the yet unanswered questions about Cu:Si(111)-(5.55×5.55).

#### ACKNOWLEDGMENTS

We are indebted to E. G. McRae and J. E. Rowe for numerous useful discussions.

- 
- <sup>1</sup>E. Bauer, *Vacuum* **22**, 539 (1972).  
<sup>2</sup>E. Daugy, P. Mathiez, F. Salvan, and J. M. Layet, *Surf. Sci.* **154**, 267 (1985).  
<sup>3</sup>H. Kemmann, F. Müller, and H. Neddermeyer, *Surf. Sci.* **192**, 11 (1987).  
<sup>4</sup>J. E. Demuth, U. Koehler, and R. J. Hamers, in *Proceedings of the Third International Meeting on Scanning Tunneling Microscopy*, 1988, Oxford, UK, edited by St. Tosch and H. Neddermeyer (unpublished).  
<sup>5</sup>R. J. Wilson, S. Chiang, and F. Salvan, *Phys. Rev. B* **38**, 12 696 (1988).  
<sup>6</sup>R. B. Doak (unpublished).  
<sup>7</sup>R. B. Doak and D. B. Nguyen, in *Proceedings of the 16th International Symposium on Rarefied Gas Dynamics*, 1988, Pasadena, California (AIAA, in press).  
<sup>8</sup>R. B. Doak and D. B. Nguyen, *Rev. Sci. Instrum.* **59**, 1957 (1988).  
<sup>9</sup>A. Guinier, *X-Ray Diffraction in Crystals, Imperfect Crystals, and Amorphous Bodies* (Freeman, San Francisco, 1963).  
<sup>10</sup>P. Bak, *Rep. Prog. Phys.* **45**, 587 (1982).  
<sup>11</sup>J. E. Demuth, U. K. Koehler, R. J. Hamers, and P. Kaplan, *Phys. Rev. Lett.* **62**, 641 (1989).  
<sup>12</sup>G. Comsa, *Surf. Sci.* **81**, 57 (1979); D. R. Frankel, *ibid.* **84**, L485 (1979).  
<sup>13</sup>K. H. Kuo, Y. C. Feng, and H. Chen, *Phys. Rev. Lett.* **61**, 1740 (1988).  
<sup>14</sup>U. Harten, J. P. Toennies, and Ch. Wöll, *Phys. Rev. Lett.* **57**, 2947 (1986).  
<sup>15</sup>O. L. Alerhand and E. J. Mele, *Phys. Rev. Lett.* **59**, 657 (1987).  
<sup>16</sup>D. M. Chen, J. A. Golovchenko, P. Bedrossian, and K. Mortensen, *Phys. Rev. Lett.* **61**, 2867 (1988); R. B. Doak (unpublished).